OLIVINE-HOSTED MELT INCLUSIONS IN OLIVINE-PHYRIC SHERGOTTITE LAR 06319. A. Basu Sarbadhikari[1,2], Y. Liu[1], J.M.D. Day[3], and L.A. Taylor[1]; [1]Planetary Geosciences Institute, Dept. of Earth & Planetary Sciences, Univ. of Tennessee, Knoxville, TN 37996, USA (amitbasu_s@yahoo.co.in), [2]The PML for Geochemistry and Cosmochemistry, Institute for Study of the Earth's Interior, Okayama Univ. at Misasa, Tottori 682-0193, Japan, [3]Department of Geology, Univ. of Maryland, College Park, MD 20740, USA

Introduction: Melt inclusions (MI) provide 'snapshots' of the magmatic conditions at the time of their entrapment, and their compositions directly record that of their parental melt during the crystallization process [1-5]. A newly-found, Antarctic, olivine-phyric shergottite, LAR 06319, contains an enriched REE signature, similar to most of basaltic shergottites [6,7]. LAR 06319 contains olivines with abundant, devitrified MI. Although these MI are devitrified, the original trapped-melt composition can be reconstructed based on mineral chemistry and modal analysis. Here, we report results on olivine-hosted MI and their implications on the evolution of the LAR 06319 parental melt.

Methodology: Analyses of major-element compositions of the minerals in MI were conducted using a Cameca SX50 electron microprobe at the University of Tennessee. Since all MI show different degrees of devitrification, modal abundances of minerals in MI were obtained by measuring the area of each mineral using image-analysis software (ImageJ, v.1.40), X-ray elemental maps and BSE imaging. Minor- and trace-element concentrations of MI were determined using a laser-ablation system coupled to an ICP-MS at the University of Maryland (details in [6]).

Inclusion Types: Based on their occurrences in the host olivine, MI of LAR 06319 are divided in three groups (details are provided in Table 1). Type-I MI occur in the core of the coarse brown olivine (Fo_{77-69}) and are generally large (~100-200 µm dia.). Type-IIa MI of intermediate size occur in olivine with Fo_{71-66}, away from the center of the coarse brown olivine. A different kind of MI is also observed to be associated with olivine of Fo_{69-68}. This MI (type-IIb) is the largest (~400 µm) of all. Unlike other types of MI with sub-rounded shape, type-IIb MI have sub-angular to angular shapes. Type-III MI are associated with olivine rims and are the smallest (~20-50 µm dia.). All MI contain pyroxenes (low-Ca and high-Ca), and glass as essential constituents, and chromite, sulfide and phosphate as accessory minerals (Table 1). Silica is only present in Type-I MI.

Composition of melt inclusions: Major-element compositions of MI are estimated from the modal abundances and average chemistry of the constituent minerals (Figs. 1-2). Post-entrapment effects on the MI was corrected for using similar methods, described in [3,4]. We estimate that addition of 15 wt.% host olivine is needed to retrieve the composition of the entrapped melt composition,

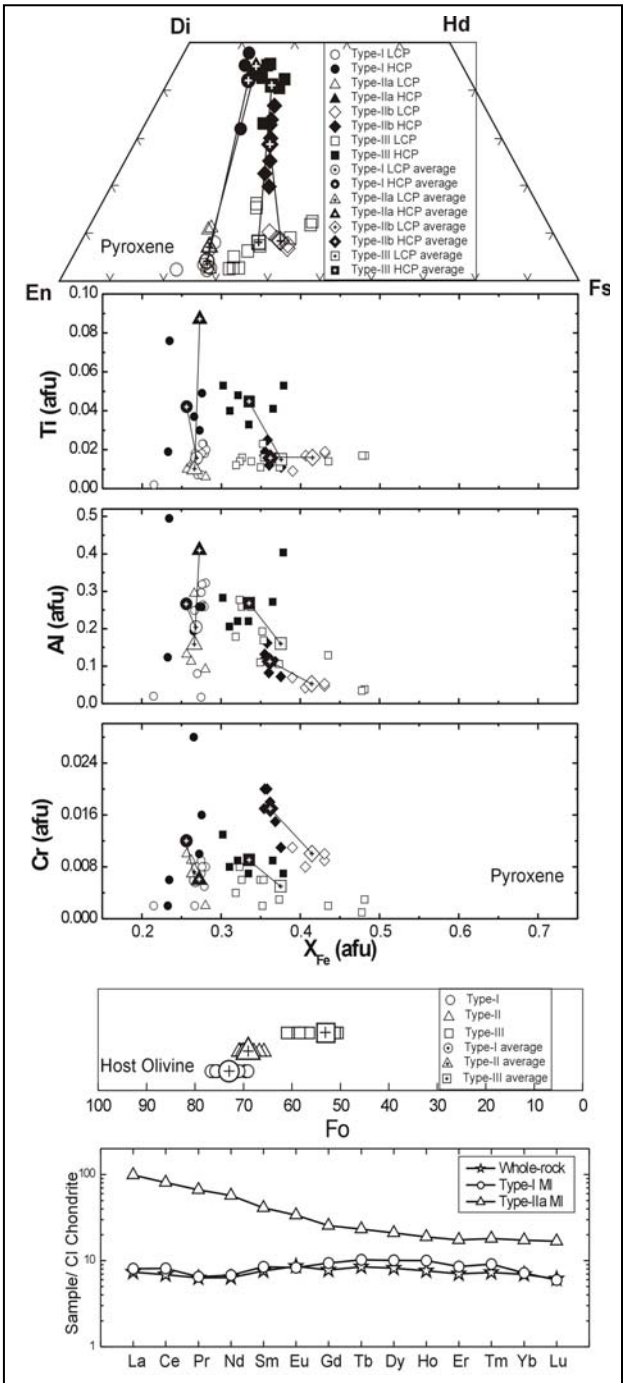

Fig. 1: Compositions of pyroxenes in MI and host olivine and CI-normalized REE patterns of Type-I & Type-IIa inclusions, as a whole.

satisfying equilibrium $K_d^{Fe\text{-}Mg}$ between entrapped melt and host olivine (Fig. 2). Type-I MI have a Mg# ~ 53, higher than that of Type-IIa MI (Mg#= 44). Trace elements were directly measured on Type-I and -IIa MI. Since the olivines contain limited incompatible elements abundances (including the REEs), corrections were not made for these data. Type-I MI have similar REEs to those of the whole-rock [6,7] (Fig. 1b). Type-IIa MI contain more REEs than Type-I MI or the whole rock (Fig. 1a).

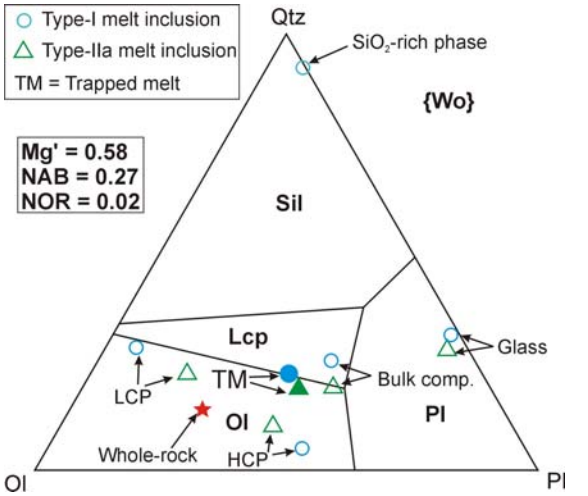

Fig. 2: Ol-Pl-Qtz system projected from Wo after [8], showing the composition of constituent minerals and the reconstructed trapped melt composition. Abbreviations: NAB, NOR = mole fractions of albite and orthoclase in the normative feldspar; Lcp, low-Ca pyroxene. Whole rock composition of LAR 06319 is from [6,7].

Discussion: The similar REE patterns between Type-I MI and that of the whole-rock for LAR 06319 [6,7] suggests LAR 06319 likely represents a melt composition. This provides powerful evidence for closed system behavior for LAR 06319 and the inheritance of incompatible-element enrichment prior to fractional crystallization. Compared to Type-I MI and the whole rock, the relatively Fe- and REE-rich Type-IIa MI are consistent with crystal fractionation. Using the highly incompatible elements (such as Rb, La), ~ 10 wt% crystals formed from the time that Type-I MI were trapped to when Type-IIa MI were trapped, which is marginally higher than that estimated from the crystallization history of the whole-rock (~ 5%) based on textural analysis [6]. This difference can be explained by subsequent crystallization of Mg-rich pigeonites in the sample, in addition to crystallization of host olivine. LAR 06319 MI preserve the petrogenetic history of the parental melt that is both complementary and consistent with the crystallization history of the sample as recorded in its minerals [6]. The earliest formed MI (Type-I) provide further evidence for incompatible-enriched mantle derived melts from the martian interior. Further work should elucidate the nature of incompatible-enrichment in both the martian crust and mantle.

References: [1] Jagoutz (1989) *GCA* 53; [2] Harvey *et al*. (1993) *GCA* 57; [3] Danyushevsky *et al*. (2000) *CMP* 138; [4] Gaetani & Watson (2002) *Chem Geol* 183; [5] Goodrich (2003) *GCA* 67; [6] Basu Sarbadhikari *et al*. (2009) *GCA*, in press; [7] Basu Sarbadhikari *et al*. (2009) this vol.; [8] Longhi *et al*. (1991) *Am Min* 76.

Table 1: Texture and composition of the constituent minerals of melt inclusions

	Type-I	***Type-IIa***	***Type-IIb***	***Type-III***
Constituent minerals	lo-Ca Px (LCP), hi-Ca Px (HCP), Glass, SiO_2-rich phase, and/or Chromite, Troilite, and Merrillite	LCP, HCP, Glass, and/or Chromite, and Merrillite	LCP, HCP, Maskelynite (Mask) and Amphibole	LCP, HCP, Glass, and/or Chromite and Troilite
Approx. mode (avg. vol.%)	**Px**: 55 {**LCP**: 10, **HCP**: 45}; **glass**: 38; **SiO_2-rich phase**: 7	**Px**: 75 {**LCP**: 15, **HCP**: 60}; **glass**: 25	**Px**: 62 {**LCP**: 14, **HCP**: 58};**Plag**: 35; **Amph**: 3	**Px**: 85 {**LCP**: 25, **HCP**: 60}; **glass**: 15
Mineral chemistry range	**Host Ol**: Fo = 69-77 **LCP**: Mg# 71-78.5; Wo# 2-8; Al_2O_3: 0.38-7.41%; TiO_2: 0.25-0.83% **HCP**: Mg# 72.5-77; Wo# 32-48; Al_2O_3: 4.34-11.2%; TiO_2: 1.06-2.70%	**Host Ol**: Fo = 66-71 **LCP**: Mg# 72-74; Wo# 2-11; Al_2O_3 2.12-6.72%; TiO_2 0.22-0.49% **HCP**: Mg# 73; Wo# 45; Al_2O_3 9.24%; TiO_2 3.08%	**Host Ol**: Fo = 68-69 **LCP**: Mg# 57-61; Wo# 6.5-10.5; Al_2O_3: 0.94-1.53%; TiO_2: 0.32-0.65% **HCP**: Mg# 62.5-64.5; Wo# 20-37; Al_2O_3: 1.59-3.58%; TiO_2: 0.38-0.86% **Mask**: $Or_{2\text{-}3}Ab_{51.5\text{-}53}An_{45\text{-}46}$ **Amph**: $^{A}(K_{0.02}Na_{0.21})_{0.23}$ $^{B}(Na_{0.29}Ca_{0.81}Mn_{0.05}Fe^{2+}_{0.85})_{2.00}$ $^{C}(Mg_{3.34}Fe^{2+}_{0.57}Fe^{3+}_{0.62}Cr_{0.02}{}^{VI}Al_{0.40}Ti_{0.04})_{5.00}Si_{6.93}{}^{IV}Al_{1.07}O_{22}(OH,F)_2$	**Host Ol**: Fo = 50.5-61 **LCP**: Mg# 52-68; Wo# 2.5-15; Al_2O_3: 0.77-5.88%; TiO_2: 0.39-0.81% **HCP**: Mg# 62-70; Wo# 33-45.5; Al_2O_3: 4.57-8.93%; TiO_2: 1.13-1.84%
Pyroxene morphology	Intergrowth of HCP within glassy mass, rimmed by LCP. Sometimes LCP also intergrows in glassy mass	Massive HCP, rimmed by LCP	HCP and LCP are intermingled at the core part; Mask and Amph occur adjacent to the inclusion wall	Patchy-type HCP rimmed by and sometimes pervaded by LCP